

Rotational modeling of Hyperion

Rebecca A. Harbison · Peter C. Thomas ·
Philip C. Nicholson

Received: 31 August 2010 / Revised: 7 February 2011 / Accepted: 15 February 2011 /
Published online: 13 March 2011
© Springer Science+Business Media B.V. 2011

Abstract Saturn's moon, Hyperion, is subject to strongly-varying solid body torques from its primary and lacks a stable spin state resonant with its orbital frequency. In fact, its rotation is chaotic, with a Lyapunov timescale on the order of 100 days. In 2005, Cassini made three close passes of Hyperion at intervals of 40 and 67 days, when the moon was imaged extensively and the spin state could be measured. Curiously, the spin axis was observed at the same location within the body, within errors, during all three fly-bys— $\sim 30^\circ$ from the long axis of the moon and rotating between 4.2 and 4.5 times faster than the synchronous rate. Our dynamical modeling predicts that the rotation axis should be precessing within the body, with a period of ~ 16 days. If the spin axis retains its orientation during all three fly-bys, then this puts a strong constraint on the in-body precessional period, and thus the moments of inertia. However, the location of the principal axes in our model are derived from the shape model of Hyperion, assuming a uniform composition. This may not be a valid assumption, as Hyperion has significant void space, as shown by its density of $544 \pm 50 \text{ kg m}^{-3}$ (Thomas et al. in *Nature* 448:50, 2007). This paper will examine both a rotation model with principal axes fixed by the shape model, and one with offsets from the shape model. We favor the latter interpretation, which produces a best-fit with principal axes offset of $\sim 30^\circ$ from the shape model, placing the A axis at the spin axis in 2005, but returns a lower reduced χ^2 than the best-fit fixed-axes model.

Keywords Chaotic motions · Extended body dynamics · Natural satellites · Satellite rotation · Hyperion principal axes

1 Introduction

Since the Voyager era, the Saturnian moon, Hyperion, has been known observationally to be a non-synchronous rotator. Wisdom et al. (1984) theoretically showed that given Hyperion's

R. A. Harbison (✉) · P. C. Thomas · P. C. Nicholson
Department of Astronomy, Cornell University, 610 Space Sciences Building, Ithaca, NY 14853, USA
e-mail: harbison@astro.cornell.edu

large resonantly-forced eccentricity and the non-spherical shape observed by Voyager, the satellite couldn't rotate synchronously and would most likely be in a tumbling state. Large portions of the phase space for its spin state, including many of the low-order spin-orbit resonances, would be chaotic with short (several orbits) Lyapunov timescales.

Despite this, several attempts have been made to model the spin of the moon over short time periods, to determine if the moon's spin state was consistent with that of a homogenous body of its shape. Klavetter (1989) was the first; using ground-based photometry and the Voyager images, he was able to produce fits consistent with a homogenous body, though the limited dimensionality of the data meant he could not guarantee that he had found a unique solution. Starting from the high-resolution Voyager images, Black et al. (1995) were able to model the low-resolution photometry obtained over 18 days prior to the encounter.

The Cassini spacecraft, in orbit around Saturn, made three close passes by Hyperion in 2005. For each fly-by, an instantaneous spin state and partial shape model were obtained (Thomas et al. 2007). Hyperion's rotational rate was observed to be between 72 and 75°day^{-1} (for comparison, Hyperion's orbital mean motion is $16.94^\circ \text{day}^{-1}$) and the spin vector was neither constant in space nor within the body. Perturbations to Cassini's orbit about Saturn required Hyperion's mean density to be a surprisingly low $544 \pm 50 \text{ kg m}^{-3}$, implying a porosity of at least $42 \pm 6 \%$, assuming pure water ice (Thomas et al. 2007).

Using these three high-resolution passes in 2005, we will search for possible fits of the moments of inertia ratios within the errors set by the shape model. Furthermore, given the porosity of Hyperion, a search for better fits, allowing for the principal axes to vary from those derived from a shape model, will also be done to look for possible large-scale inhomogeneities caused by voidspace or regions of solid ice.

2 Data

From the current shape model (Thomas et al. 2007), and assuming a homogenous interior, we obtain dimensionless moments of inertia $A = 0.314 \pm 0.010$, $B = 0.474 \pm 0.008$, and $C = 0.542 \pm 0.008$ in units of $M \langle R \rangle^2$, where M is the mass of Hyperion and $\langle R \rangle$ is mean radius ($135 \pm 4 \text{ km}$). This gives $A/C = 0.58 \pm 0.03$ and $B/C = 0.87 \pm 0.03$.

Tables 1 and 2 give data previously presented in Black et al. (1995) and Thomas et al. (2007), as well as 2007 observations first presented in this paper, but obtained by the same methods as used in Thomas et al. (2007). Osculating orbital elements for Hyperion were obtained from JPL's HORIZONS database, and were calculated via numerical integration with initial conditions taken from Jacobson (1996).

Some things are readily apparent from these instantaneous spin states. During all five close fly-bys, Hyperion was observed in a similar state, that of non-principal axis rotation with a spin axis closest to the long shape axis (presumably corresponding to the A principal axis), and 4.2 to 4.4 times faster than synchronous. The three 2005 observations show the same in-body location of the spin axis within errors, though it has moved between 1981, 2005 and 2007. Rotation about the A axis would be dynamically stable when it comes to free-body rotation, but under dissipation and without strong forcing, the rotation should shift to the minimum energy state about the C axis. Indeed, this is what most natural satellites show. However, Black et al. (1995) did perform long-term ($\sim 10^6$ orbit) integrations, showing that the near-A-axis rotational state seen in 1981 (and 2005, and 2007) was not unusual for Hyperion. A similar quasi-stability was seen in rotational models of Prometheus and Pandora done by Melnikov and Shevchenko (2008), where even chaotic solutions to the moons' rotation have a preferred orientation.

Table 1 Initial conditions of the orbit and spin at the mid-point of each fly-by. The values of e , ϖ and M were used to derive the distance to Saturn (r) and the true anomaly, f

Date	e	ϖ	M	θ_0	ϕ_0	ψ_0	$\omega_A / \omega $	$\omega_B / \omega $	$\omega_C / \omega $	$ \omega $
2005-06-10	0.115	105°	295°	0.004	1.441	0.427	0.890	0.067	0.451	4.433
2005-08-16	0.115	102°	342°	1.885	2.118	1.180	0.907	0.162	0.389	4.255
2005-09-25	0.113	99°	303°	2.989	1.685	1.641	0.902	0.133	0.411	4.255

θ , ϕ and ψ are the calculated Euler angles describing the change of coordinates from the Saturn-centric coordinate system (used to find the influence of torques from Saturn) to the body-centric principal-axis coordinate system (see Sect. 3 and Black et al. 1995), and the ω 's are the angular velocity (in units of orbital frequency) about each of the shape-determined principal axes

Table 2 Rotation state observed during all close flybys of Hyperion, including results presented in Thomas et al. (2007) and Black et al. (1995)

Date	$\omega_A / \omega $	$\omega_B / \omega $	$\omega_C / \omega $	ω_x	ω_y	ω_z	$ \omega $ (° d ⁻¹)	σ_ω (°)
1981-08-23	0.986	0.160	-0.049	-2.457	-2.501	2.409	72 ± 3	10
2005-06-10	0.890	0.067	0.451	3.399	-1.511	2.411	75 ± 1	2
2005-08-16	0.907	0.162	0.389	3.026	1.909	2.303	72 ± 1	4
2005-09-25	0.902	0.133	0.411	1.151	2.018	3.565	72 ± 1	10
2007-02-16	0.749	0.080	0.659	-3.797	1.905	0.250	72 ± 1	10

Angular velocity measured both in the body-centric frame and in the xyz quasi-inertial coordinate frame, with z as the direction of Saturn's pole, x as the direction from Saturn towards Hyperion's pericenter at the time of the observation, and y chosen to form a right-handed coordinate system. All results in the ABC frame, save the 1981 data, were calculated with the current shape model; the 1981 data are taken directly from Black et al. (1995), and used the Voyager-era shape model. The total spin frequency (in units of orbital frequency) is also noted, with estimates on the error, as is the error in position of the spin axis in inertia space (in degrees)

Movement of the spin axis in inertial space is also evident, and obvious even on the 40–70 day timescale between the 2005 fly-bys. Again, unlike the minimum-energy Cassini state occupied by more regular satellites, Hyperion's spin axis is not confined to near the orbit normal (here, the z axis). Black et al. (1995)'s models showed the expected forced nutation and precession about the orbit normal with a 300-day period, as well as a shorter 10–20 day precession about the A axis, and the 100-day span between the 2005 observations would easily show these motions.

3 Dynamical modeling

The model used to calculate the rotation is a six-dimensional system of differential equations, with three coordinates tracking the angular orientation of Hyperion in space, and three tracking the angular velocity of Hyperion's spin. The full system of equations of motion, taken from Black et al. (1995), is:

$$\dot{\phi}_E = \frac{\omega_A \sin \psi_E + \omega_B \cos \psi_E}{\sin \phi_E} \quad (1)$$

$$\dot{\psi}_E = \omega_A \cos \psi_E - \omega_B \sin \psi_E \quad (2)$$

$$\dot{\psi}_E = \omega_C - \dot{\phi}_E \cos \phi_E \quad (3)$$

$$\dot{\omega}_A = \frac{B - C}{A} \left(\omega_B \omega_C - \frac{3\beta\gamma}{r^3} \right) \quad (4)$$

$$\dot{\omega}_B = \frac{C - A}{B} \left(\omega_A \omega_C - \frac{3\alpha\gamma}{r^3} \right) \quad (5)$$

$$\dot{\omega}_C = \frac{A - B}{C} \left(\omega_A \omega_B - \frac{3\alpha\beta}{r^3} \right) \quad (6)$$

We use the conventional Euler angles $(\theta_E, \phi_E, \psi_E)$ to specify angular position of Hyperion's principal axes, which were computed from the current shape model and the assumption of constant density, relative to the xyz axes. Because the Euler angles have a singularity when $\sin \phi$ approaches 0, a transformation to Wisdom's alternate angular coordinates (a set of angles where the third rotation is about the y axis, rather than the z axis used in conventional Euler angles) is made when $|\sin \phi_E| \leq 10^{-6}$ and we return to the conventional Euler angles when $|\cos \phi_W| \leq 10^{-6}$ (Wisdom et al. 1984). The transforms are:

$$\tan \theta_W = \frac{\cos \theta_E \sin \psi_E + \sin \theta_E \cos \phi_E \cos \psi_E}{\cos \theta_E \cos \phi_E \cos \psi_E - \sin \theta_E \sin \psi_E} \quad (7)$$

$$\tan \phi_W = \sin \phi_E \cos \psi_E \quad (8)$$

$$\tan \psi_W = \frac{-\sin \phi_E \sin \psi_E}{\cos \phi_E} \quad (9)$$

$$\tan \theta_E = \frac{\cos \theta_W \sin \psi_W + \sin \theta_W \sin \phi_W \cos \psi_W}{\cos \theta_W \sin \phi_W \cos \psi_E - \sin \theta_W \sin \psi_W} \quad (10)$$

$$\tan \phi_E = \frac{1}{\cos \phi_W \cos \psi_W} \quad (11)$$

$$\tan \psi_E = \frac{-\cos \phi_W \sin \psi_W}{\sin \phi_W} \quad (12)$$

Unlike previous work (Wisdom et al. 1984; Black et al. 1995; Melnikov and Shevchenko 2008), instead of using the derivatives of Euler angles with respect to time as our measure of angular velocity (and thus using equations for the second derivatives of Euler angles to compute the changes in angular velocity), we use the instantaneous angular velocities about the principal axes, ω_A , ω_B and ω_C . This reduces the number of coordinate changes should the problem approach the singular situation of $\sin \phi_E = 0$, and eliminates the need to convert derivatives of Euler angles into a more physically intuitive coordinate system for display.

The angles α , β , and γ in Eqs. 1–6 are the direction cosines from the principal axes to the instantaneous direction of Saturn, defined as (Black et al. 1995)

$$\alpha = \cos(\theta_E - f) \cos \psi_E - \sin(\theta_E - f) \cos \phi_E \sin \psi_E \quad (13)$$

$$= \cos(\theta_W - f) \cos \psi_W - \sin(\theta_W - f) \sin \phi_W \sin \psi_W \quad (14)$$

$$\beta = \cos(\theta_E - f) \sin(-\psi_E) - \sin(\theta_E - f) \cos \phi_E \cos \psi_E \quad (15)$$

$$= \sin(\theta_W - f) \cos \phi_W \quad (16)$$

$$\gamma = \sin(\theta_E - f) \sin \phi_E \quad (17)$$

$$= \cos(\theta_W - f) \sin \psi_W + \sin(\theta_W - f) \sin \phi_W \cos \psi_W, \quad (18)$$

where f is the true anomaly of Hyperion in its orbit. A , B and C are the values of the shape-derived moments of inertia, and r is the distance between Hyperion and Saturn (in units of $a = 1$). Time is measured in units of $P_{Hyp} = 2\pi$, so that the orbital angular velocity,

$n = 1$, and the spin angular velocities are thus measured in multiples of n . In physical units, $P_{Hyp} = 21.43$ days and $a = 1.484 \times 10^6$ km, or 24.6 Saturn radii.

The orbit of Hyperion is modeled as a static (non-precessing) ellipse about a spherical planet in the equatorial plane. Hyperion's orbital inclination is small, and it is sufficiently far from Saturn that its apsidal precessional period due to Saturn's oblateness—the pericenter moves 6° between June and September 2005—is long compared to the spin, orbital and Lyapunov timescales. Hyperion is in a 3:4 orbital resonance with Titan, which forces additional variations in its eccentricity and longitude of pericenter (Peale 1999), but the 18.8 year variation in eccentricity (Duriez and Vienne 1997) again occurs over a much longer timescale than our integrations of its spin state.

The integration of the system of Eqs. 1–6, as well as Hyperion's orbital position and velocity was performed using a fourth-order Runge-Kutta algorithm. The initial conditions, which are presented in Table 1, are set by the observations during one of the close fly-bys of Hyperion by Cassini. Initially, the middle observation was used, and the integration was performed in two directions. However, further data analysis showed that the first (June) observation had the lowest uncertainty in spin axis direction and this datum was settled upon as the initial conditions for all runs mentioned in this text. At each step, the orbital position and velocity were calculated using Newton's Laws and substituted into the rotational equations to calculate the torques from Saturn.

Step size was chosen as a compromise between speed of integration and accuracy, and was varied between runs—integrations which need not be compared to data used a step size of $\pi/400$ (1/800th of an orbit, or approximately 1/160th of a rotation), while integrations fitted to the three Cassini observations were subdivided into 5000 steps between June and August (or a step size of 6.28×10^{-4} of an orbit), and another 5000 steps between August and September (or a step size of 3.78×10^{-4} of an orbit). Tests using larger and smaller step sizes produced comparable results, with steps a quarter, a half and double the length not producing quantifiably different (within the output precision) results, while steps four times as long showed less than one part in 10^4 difference in spin rate over 100 days.

As a test of our integration code and in order to find the Lyapunov timescale, the inputs were perturbed by one part in 10^{12} and four integrations offset in different directions in parameter-space from a fifth were compared for a period of 800 days. The difference in Euler angles and angular velocities between one such run and the 'reference' integration are plotted versus time in Fig. 1, where they show a good fit to the chaotic behavior expected, growing exponentially with respect to time (and appearing linear in the semi-log plot). Fitting the slope of the divergence between solutions with respect to time to an exponential function returns a Lyapunov time of 61.4 ± 3.6 days. While this timescale is slightly longer than that reported by Wisdom et al. (1984), who assumed a near-synchronous initial state, they do show that dynamical models cannot be expected to be predictive over a period of more than a few months.

The first run of the model started from the June 2005 (Day 161) fly-by, and extrapolated Hyperion's rotation forward (and backward) in time. The reported error of the spin axis's position is 2° in the June 2005 measurement, as seen in Table 2. Given the measured Lyapunov timescale, the error in the predicted spin axis direction should grow to 6° at the time of the August fly-by and 11° in September. Both of these numbers are larger than the uncertainties in the observations, but not significantly so, making it possible to compare the observations with the model's results as long as the effects of the chaos are kept in mind.

The results, shown by the magnitude of the spin and the decomposition of the spin along the shape model's axes, are plotted versus time in Fig. 2. Note that the spin rate predicted by the model fits the September 2005 (day 268) datum quite well, though it is noticeably

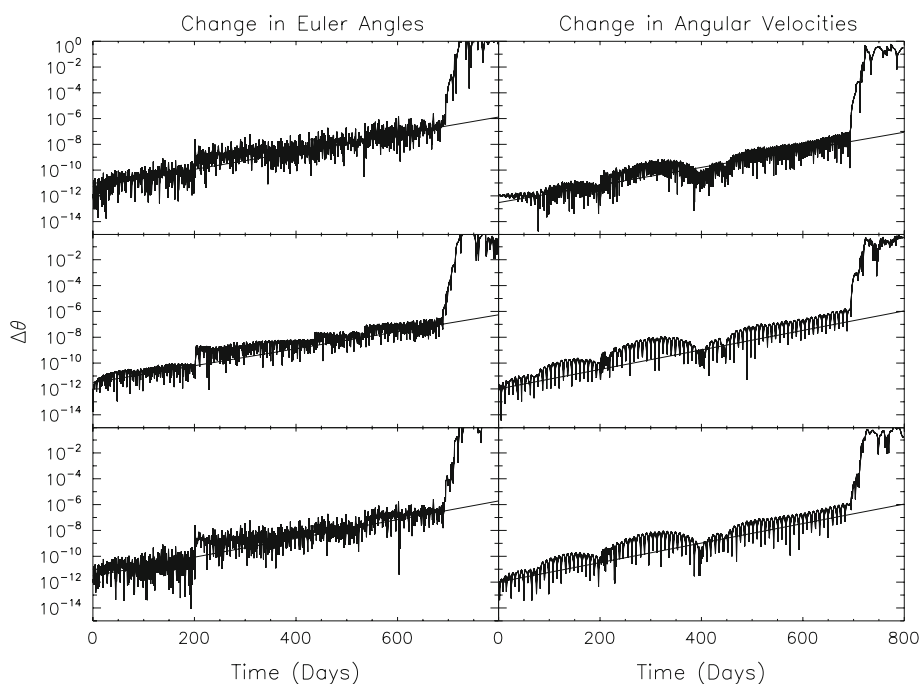


Fig. 1 Relative differences in rates and principal axis orientations ω and θ as functions of time (in days), starting from a difference of 10^{-12} (machine double precision). The behavior for the first 700 days is roughly exponential, as expected for a chaotic system, with similar Lyapunov exponents, producing a mean exponential-growth timescale of 61.4 ± 3.6 days

different than the August 2005 (day 228) observation. However, the position of the spin axis within the body—as seen in the decomposition of the spin rate into its A, B, and C components—does not match the observations well. It is observed to stay relatively fixed, while the model predicts it to precess about the A axis, with a period of about 16 days. This was also seen by [Black et al. \(1995\)](#), who calculated a theoretical free precession period of 15.2 days. This motion can better be seen in a polar plot, such as Fig. 3.

Figure 3 depicts the positions of the spin poles observed during all close fly-bys of Hyperion, in addition to the trace of the pole position from the simulation shown in Fig. 2. Note that the free precession is about the A axis, as one would expect for an ellipsoid that is nearly a prolate spheroid. The torques from Saturn do not change the general behavior on this timescale. Also note how far the 2007 point is from the no-torque-equilibrium point of either A-axis or C-axis rotation, confirming that Hyperion is in a state of non-principal axis rotation.

Figure 4 unfolds the simulation trajectory plotted in Fig. 3 and plots it and the spin rate with respect to time. Though the error is large in the latitude of the spin axis, the measured latitudes are consistent with the model. However, this plot shows vividly the 180° discrepancy in the longitude of the September 2005 point, and $\sim 120^\circ$ in August of 2005. This suggests that the assumption that Hyperion is a uniform-density body whose mass distribution can be derived from the shape model should be examined further, to see if an acceptable solution can be found within the errors of the observations and shape model.

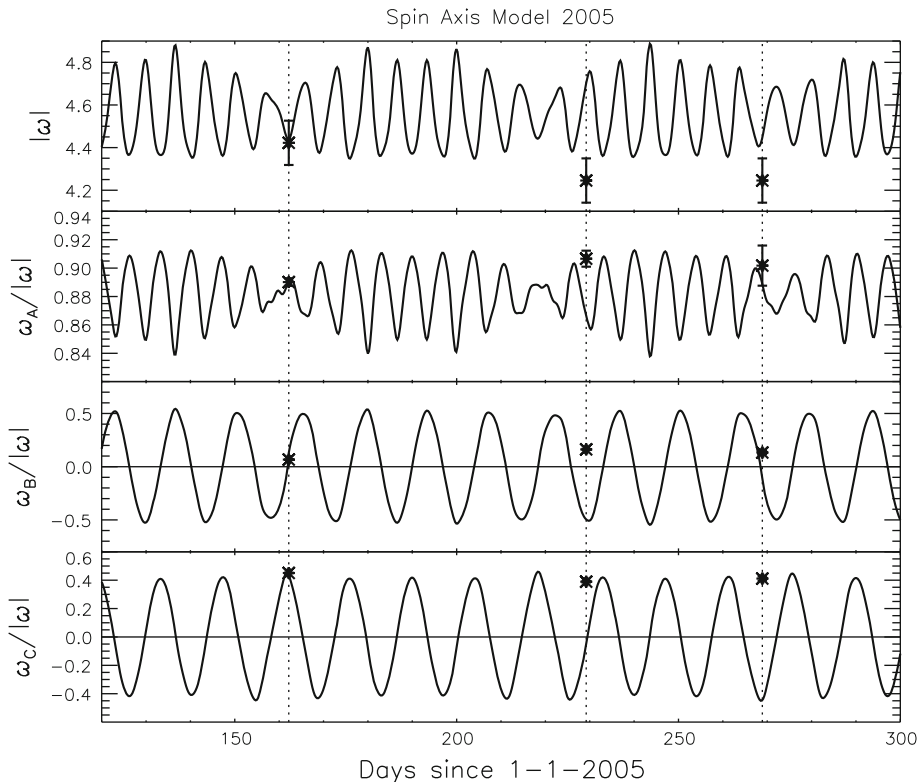


Fig. 2 Model of the spin rate and position of the spin axis in body-centric coordinates—using as measures the component of spin around each principal axis—starting from the June 2005 observation and progressing forward and backward for approximately 140 and 50 days respectively, using the [Thomas et al. \(2007\)](#) values for A, B, and C. All three observations are marked as points on the graph. Note the predicted period of about 16 days in ω_B and ω_C and 8 days in ω_A , and the near-identical values of the three observations compared to the large variations in ω_B and ω_C predicted by the integration

4 Varying the initial conditions and moment ratios

The rotational pole of Hyperion was observed to move less than 10° with respect to the surface between the three 2005 flybys (Fig. 3). But the spin axis should be freely precessing around the A axis as it rotates, as shown in the model. Two explanations for this make dynamical sense: either the spin axis is closer to the true A axis, making the amplitude of precession less than observational error, or that the three observations happen to be separated by roughly integer multiples of the precessional period. The precessional period is affected by the moments of inertia, the rotation rate, and the offset between the spin axis and axis of precession, while the position of the spin axis relative to the principal axis will affect the amplitude of precession.

In this section, we explore the parameter space, varying the spin axis, spin rate and moment of inertia ratios, to see which solutions consistent with the estimated error bars might bring the spin axis back to the same position at each close fly-by of Cassini. We assume fixed locations of the principal axes based on the [Thomas et al. \(2007\)](#) shape model with a homogenous interior.

Fig. 3 A projection of the spin axis into a body-centric coordinate frame, with a pole at the shape-defined A (*long*) axis of the body, and the x axis set by the shape-defined C (*short*) axis. Observations are marked with stars, while the projected 100-day path of the spin pole within the body, as plotted in Fig. 2, is marked with a *black line*—the period is roughly 16 days

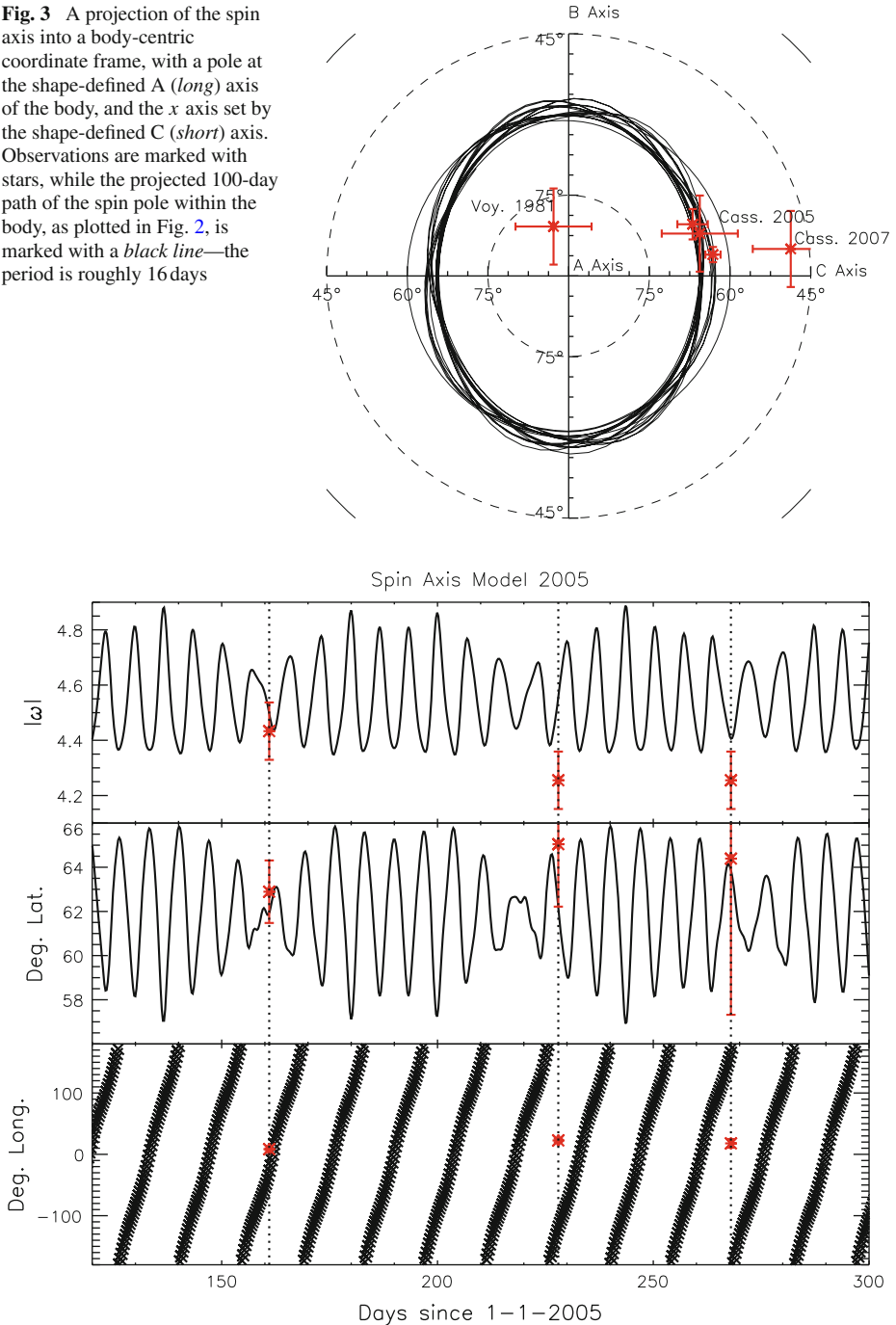


Fig. 4 Figure 3 unfolded in time, and plotted in units of body-centric latitude and longitude (with the A axis as the pole and the A-C meridian marking 0 degrees longitude) and spin rate. Note that the data (*stars*) show that the latitude is consistent with the shape-derived model (*line*), but not the longitude

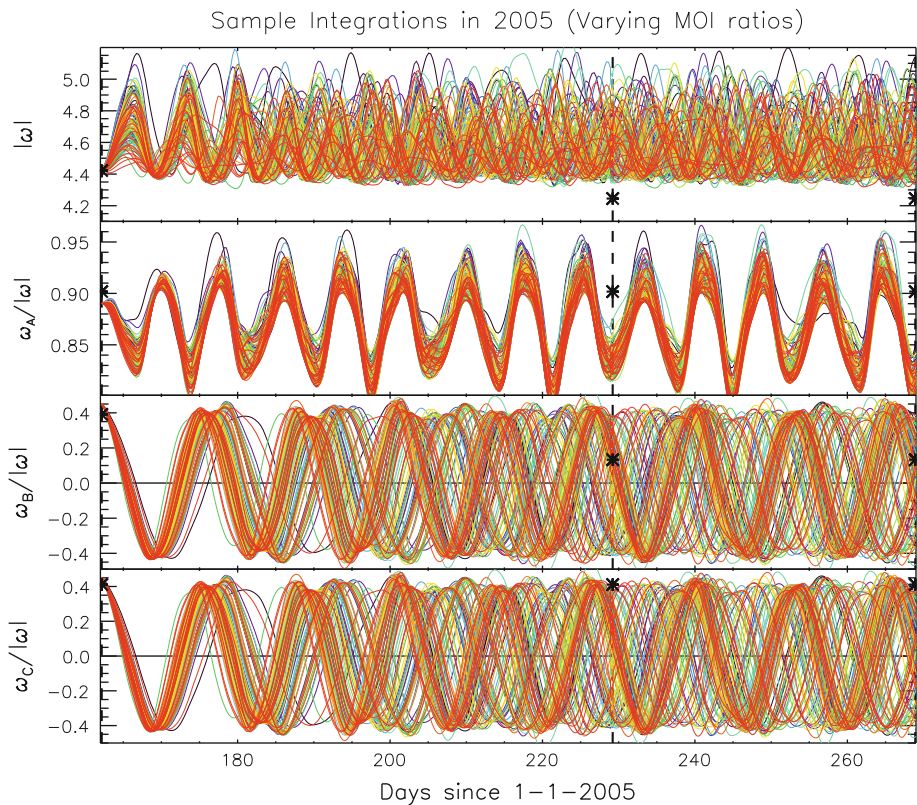


Fig. 5 Model of the position of the spin axis and magnitude of Hyperion's spin in body-centric coordinates, starting from the June 2005 point and progressing forward in time for 107 days. All three Cassini observations are marked as *asterisks* on the plot. The moments of inertia were given random Gaussian errors of $\sigma = 0.027$ for A/C and B/C, while the initial spin state was held as observed. The principal effect of changing the moments of inertia seems to be a variation in the precessional period (as seen in the phase shift in the rotation about the B and C axes), with some variation in the amplitude of the periodic oscillations. 100 trajectories are plotted

Two sets of model integrations were done, one in which only the spin axis was allowed to vary within the estimated errors in the data, and one in which only the moments of inertia were allowed to vary. To quickly sample a multi-dimensional parameter space, a random value was chosen for each parameter, using a Gaussian distribution with the nominal value as the mean and the estimated observational or modeling error as the standard deviation. The set of 100 results for the variation in the moments of inertia (or more properly, their ratios, A/C and B/C) can be seen in Fig. 5, and the 100 results for the variations in position and magnitude of the June 2005 spin vector can be seen in Fig. 6.

The nominal model rotates primarily about the A-axis. This is unusual for a rotating body in general, as it is not as energetically stable as rotation about the C-axis. However, this was also the state observed by Voyager 2. Varying the moments of inertia (Fig. 5) does not seem to change this rotational state. However, it does have the desired effect on the precessional period, changing it to produce possible returns to the June location of the spin pole during the other fly-bys. Changing the initial spin state within observational errors (Fig. 6) produces an effect of similar magnitude. The primary effect here is of moving the spin axis towards or

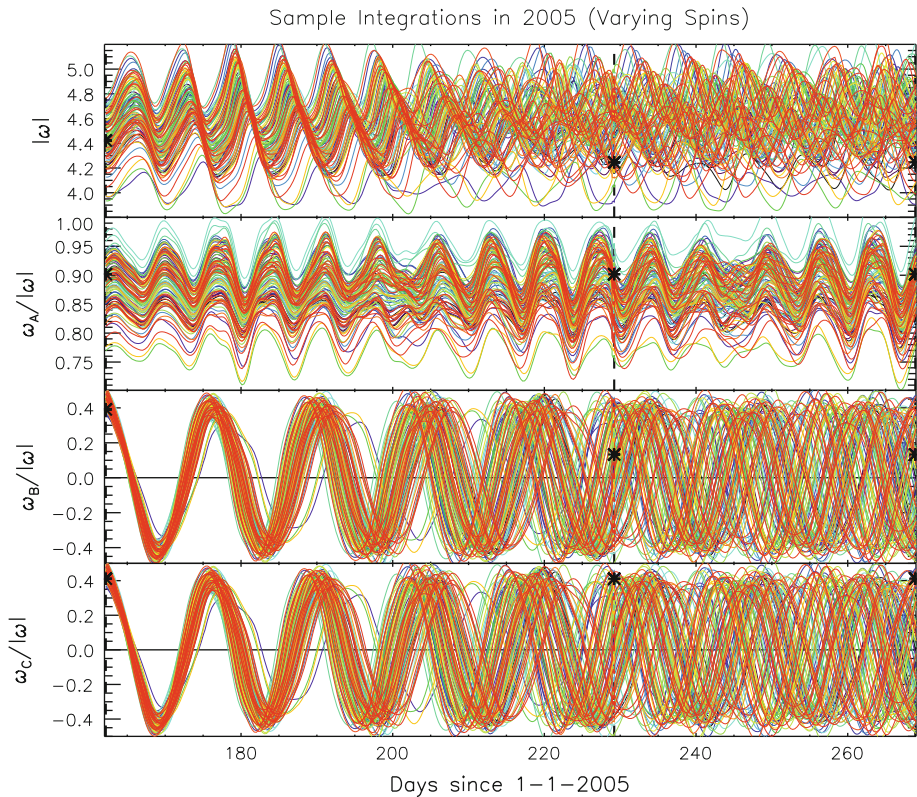


Fig. 6 Model of the position of the spin axis and magnitude of Hyperion's spin in body-centric coordinates, starting from the June 2005 point and progressing forward in time for approximately 107 days. All three Cassini observations are marked as *asterisks* on the plot. The spin magnitude was given a random Gaussian error of $\sigma = 0.047n$ (1° per day). The error in spin direction was given a random Gaussian error of $\sigma = 2^\circ$. The moments of inertia were held constant at the ones derived from the shape model. 100 trajectories are plotted

away from the axis of precession, with a corresponding change in the amplitude of precession about the A axis and the wobble towards and away from the A axis.

Although all three measurements of ω_A , ω_B and ω_C appear to be within the ranges of our solutions, two or three-dimensional cuts through parameter space such as these do not tell the whole story. While Figs. 5 and 6 show that the individual components of the spin vector in August and September can be reached within their uncertainties from the June measurement, it does not answer the question of whether the full six-dimensional spin states are recovered. We will address better methods to examine this issue in the next section.

5 Limits on the moments of inertia

As the model demonstrates, Hyperion's spin axis has two motions within the body on 100-day timescales—a small 'wobble' in the spin axis towards and away from the A axis, and a precession of the spin axis around the A axis, with the precession being the larger motion. Black et al. (1995) give an exact expression for the spin axis's free precessional period in their Eq. 8, but, given the near-equality of B and C, the assumption of a prolate spheroid

should produce a reasonable approximation. The precessional period of the spin axis within the body, given $\omega_{rot} = \frac{2\pi}{P_{rot}}$, for a prolate spheroid is (Fowles and Cassiday 1999):

$$P_p = \frac{\bar{C}}{\bar{C} - A} \frac{P_{rot}}{\cos \delta} \quad (19)$$

where $\delta \approx 30^\circ$ is the angle between the spin axis and the A axis, and \bar{C} is the geometric mean of the B and C moments. Note that this is distinct from the forced precession of Hyperion's spin axis in inertial space due to the mean torque from Saturn, whose period is on the order of 200–300 days (Black et al. 1995).

If we re-write this equation in terms of the moment of inertia ratios, rather than their individual values, we get

$$P_p = \frac{\sqrt{B/C}}{\sqrt{B/C} - A/C} \frac{P_{rot}}{\cos \delta} \quad (20)$$

or

$$B/C = \frac{(A/C)^2}{\left(1 - \frac{P_{rot}}{P_p \cos \delta}\right)^2}. \quad (21)$$

From this expression, and assuming that $\delta \approx 28^\circ$ (from Fig. 4) and an average rotational frequency of $4.5n$, the expected precessional period for the nominal moments of inertia derived from the shape model is 15.1 days. This compares well to the precession seen in the model, and agrees almost exactly with Black et al. (1995)'s more precise calculation. Given a tweaked precessional period—say, one for which small integer multiples were equal to the intervals between successive fly-bys of 40 and 67 days—one could work backward to determine a function of B/C versus A/C that would produce that period. Should such a solution exist, this would neatly solve the matter of whether Hyperion's spin axis could have been observed at the same position during all three 2005 fly-bys.

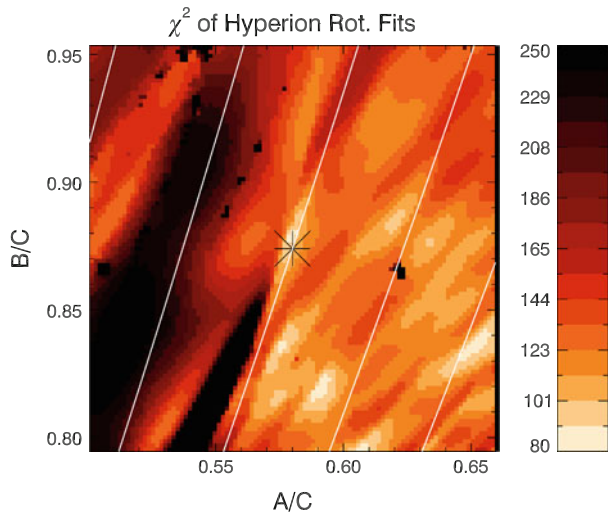
In reality, of course, this is a simplification. Hyperion's triaxial shape means that the above calculation is but an approximation to reality, and there are other factors not considered here—Hyperion's instantaneous spin rate is changing and the pole is wobbling within the body. But this gives a conceptual idea of what dominates the fitting process.

In order to do a more detailed analysis, we divided the A/C and B/C parameter space into a 30 by 30 grid centered on the shape-model's estimate and scaled so the search space was six σ by six σ (or 0.18 by 0.18), and integrated each curve from the June 2005 observation forward to August 2005 and September 2005. The resulting spin state were then compared to the observations by the function

$$\chi^2 = \sum \frac{|\omega - \omega_0|^2}{3|\omega|^2 \sigma_\omega^2} + \frac{3 - (\mathbf{A} \cdot \mathbf{A}_0^2 + \mathbf{B} \cdot \mathbf{B}_0^2 + \mathbf{C} \cdot \mathbf{C}_0^2)}{3\sigma_\theta^2} \quad (22)$$

where \mathbf{A} , \mathbf{B} and \mathbf{C} are the principal axis vectors as predicted from the model, ω is the vector composed of ω_A , ω_B , and ω_C , predicted from the model, and ω_0 , \mathbf{A}_0 , \mathbf{B}_0 and \mathbf{C}_0 are those observed. σ_ω and σ_θ represent the angular errors in the spin axis and body orientation, respectively. The χ^2 is summed over all observations excluding the initial conditions of the integration. In this case, that means summing the August and September 2005 observations, but not those from June 2005.

Fig. 7 The χ^2 of the observed rotation states in August and September 2005 given the rotation state in June 2005 as a function of A/C and B/C. *Lighter shading* indicates lower values of reduced χ^2 , and the *star* in the center of the diagram marks moments derived from the shape model. For reference, the plot is 6 times larger than the estimated errors in A/C and B/C. The model was smoothed with a median filter to eliminate spurious results. Parabolas are *lines* of theoretical constant precessional period, plotted at semi-regular intervals (This figure is in colour in the electronic version)



From Eq. 21, we would expect that curves of constant precessional period will be parabolas in A/C versus B/C space. Given the modest uncertainties in the measurements, the parabolas of equal precessional period should be picked out strongly in A/C versus B/C space, with those that produce near-integer periods of precession between the pairs of observation producing low χ^2 valleys, and those that have half-integer periods between one or both pairs producing high χ^2 peaks.

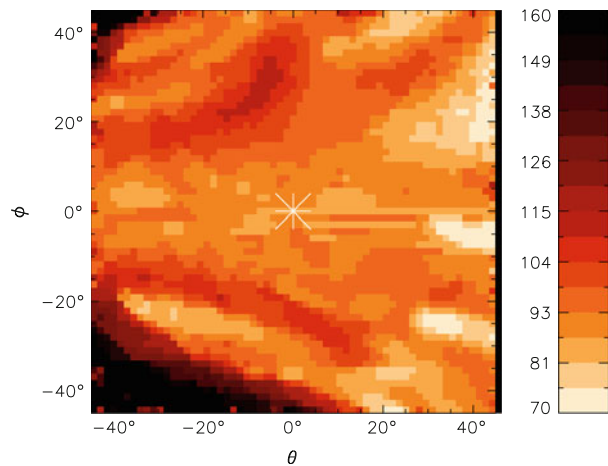
The results, smoothed by a median filter and plotted as a contour plot of A/C versus B/C can be seen in Fig. 7. There is a local minimum near the shape-derived values of the moments of inertia with a reduced χ^2 (with 10° of freedom) of 80. As mentioned above, the precessional period at the local minimum near the shape-derived moments of inertia has a period of approximately 15.1 days. Remembering that the later two fly-bys in 2005 were 67 and 107 days from the first fly-by, this yields intervals of 4.4 and 7.0 periods between flybys.

There is a similarly-deep minimum at $A/C \approx 0.61$; $B/C \approx 0.80$, as well as other noteworthy minima in the lower-right quadrant of the figure. The local minimum at $A/C=0.61$, $B/C=0.80$ gives a precessional period of 18.0 days, giving intervals of 3.7 and 5.9 periods between the first and subsequent flybys.

As expected from Eq. 21, areas of good and bad fits follow curved shapes, though not quite the predicted parabolas (plotted in white in Fig. 7). Both solutions mentioned above yield a near integer-number of precessional periods between June and September, but a non-integer between June and August. Integrating the position of the spin axis at these minima confirms that there are a whole number of cycles of precession between the first and last fly-bys.

The more detailed integration does correspond with our naive expectation that the best-fit models would be ones where precession returns the spin axis to the same position during each fly-by. However, the parameter search did not produce a solution that would return the location of the August 2005 spin axis relative to the surface to its June location. Our integrations held the June 2005 spin vector fixed as the initial conditions; allowing this to vary might produce better fits, but the exponential growth in the spin axis uncertainty due to chaos rapidly overwhelms any plausible initial error. On the other hand, we must consider the possibility that merely adjusting the moments of inertia is not enough to produce a good fit to the data.

Fig. 8 The χ^2 of the observed rotation states in August and September 2005 given the rotation state in June 2005 as a function of the Euler principal-axis-offset angles θ and ϕ , and minimized along ψ . The star in the center of the diagram marks the principal axis locations derived from the shape model, and lighter shading indicates a lower reduced χ^2 . The model was smoothed with a median filter to eliminate spurious results, which raised the plotted χ^2 in local minima (This figure is in colour in the electronic version)



6 Variations in orientation of the principal axes

Our nominal model assumes a homogenous Hyperion to calculate the moments of inertia, which are then used in the rotation model to evolve the spin states between flybys. While the models in Fig. 7 relax the assumption of homogeneity, we have still assumed that the principal axes lie along the long and short symmetry axes of the shape model. However, that need not be the case.

Hyperion is known to have a large degree of voidspace (Thomas et al. 2007), which indicates that it is a mix of solid material, most likely an ice mixture at densities around 1000 kg m^{-3} , and empty space. While a simple inhomogeneous density model (for example, a density increase towards the center) might result in a change in the moment ratios without a change in the principal axes from a homogenous model, an asymmetric distribution of voidspace would produce changes in both.

In order to simulate an offset from the shape model axes, a second set of Euler angles was specified and then the long and short shape-model axes and the spin axes were rotated through these angles. This represents a shift in the true principal axes from the ones derived from the shape model. These angles were selected to be within 45° of the (0,0,0) triplet of angles that specified that the shape axes were identical to the principal axes. The differential equations were then integrated starting from the June 2005 body orientation and instantaneous spin state, and the transformation was then done in reverse to compare the final spin state and body orientation to the right ascension and declination observations of the shape and spin axes.

While the Euler angles cannot be visualized as a physical location of the principal axes in space without a conversion, as offsets in right ascension and declination might be, they are easier to sample in a uniform manner. This gives a 3-dimensional phase space within to search for the best fit to the data. For ease of display, the minimum of each 2D sub-space is plotted in Figs. 8, 9 and 10, with the χ^2 calculated as specified in Eq. 22.

As Figs. 8, 9 and 10 show, there is a large minimum in phase space that is located some tens of degrees from the principal axes derived from the shape model, near $\theta' = 40^\circ$, $\phi' = 20^\circ$, $\psi' = 10^\circ$. This is deeper than the minima seen in Fig. 7, with a reduced χ^2 of 57, significantly less than the ~ 80 when only the moment of inertia ratios were adjusted.

Using the position of the principal axes after the rotation from the shape axes, we can reproject Figs. 8, 9 and 10 to a more physically-meaningful coordinate system. This was done in Fig. 11, which plots the location of the A axis (i.e., the minimum moment of inertia)

Fig. 9 The χ^2 of the observed rotation states in August and September 2005 given the rotation state in June 2005 as a function of the Euler principal-axis-offset angles θ and ψ , and minimized along ϕ . The *star* in the center of the diagram marks the principal axis locations derived from the shape model, and *lighter shading* indicates a lower reduced χ^2 . The model was smoothed with a median filter to eliminate spurious results, which raised the plotted χ^2 in local minima (This figure is in colour in the electronic version)

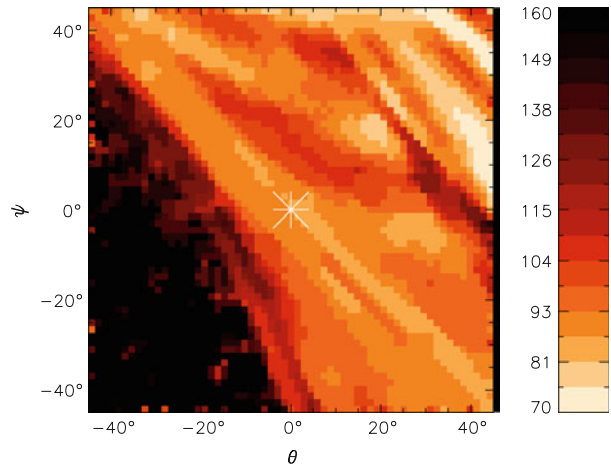


Fig. 10 The χ^2 of the observed rotation states in August and September 2005 given the rotation state in June 2005 as a function of the Euler principal-axis-offset angles ψ and ϕ , and minimized along θ . The *star* in the center of the diagram marks the principal axis locations derived from the shape model, and *lighter shading* indicates a lower reduced χ^2 . The model was smoothed with a median filter to eliminate spurious results, which raised the plotted χ^2 in local minima (This figure is in colour in the electronic version)

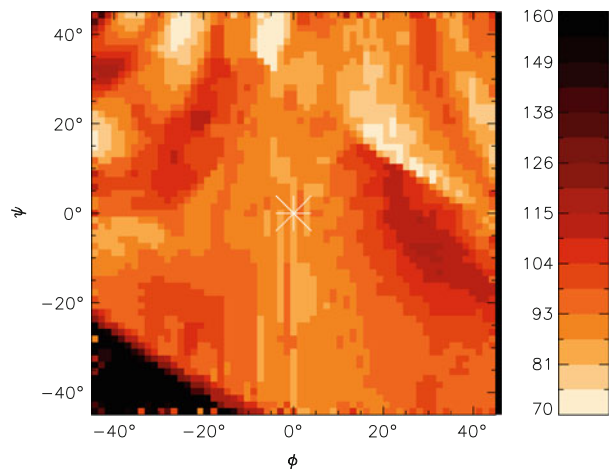
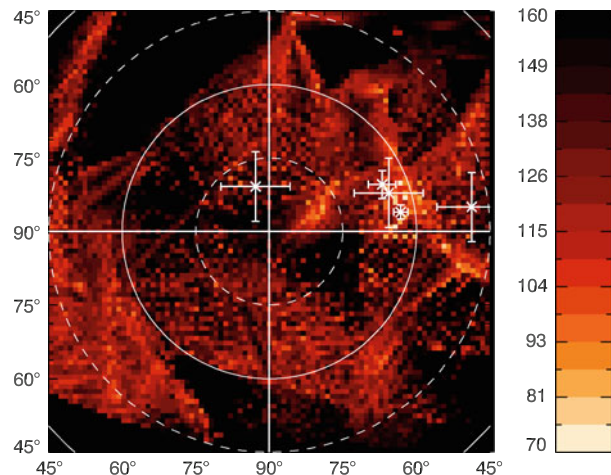


Fig. 11 The data from Figs. 8, 9 and 10, reprojected to show the location of the A axis, relative to the shape-derived *a* axis (90° latitude) and *c* axis (0° latitude, 0° longitude). The *stars* with *error bars* marks the location of the spin axes, seen in 1981 (*leftmost*), 2005 (*center cluster*) and 2007 (*right*). Note the deep minima from Figs. 8 through 10 place the preferred location of the A axis almost directly beneath the location of the spin pole in 2005 (This figure is in colour in the electronic version)



in terms of the body-centric coordinate system used previously in Fig. 3, where the pole of the plot is the shape-derived A axis, and 0° longitude is the location of the shape-derived C axis. Here the location of the deep minimum, indicating the best fit of the actual A axis, seems to be very near the location of the spin pole observed in 2005, some 30° from the shape-derived *a* axis. This is what one would expect in order to minimize in-body precession without relying on specific moment ratios to make the intervals between flybys match the precessional period.

7 Conclusions

At the time of the Cassini fly-bys in 2005, Hyperion was found in a state of non-principal axis rotation, with the spin axis nearly coincident with the long shape axis and a spin period 4.2 to 4.5 times synchronous, similar to what was observed during the Voyager flyby, and again by Cassini in 2007. Modeling suggests that this state is in fact more stable than a near-synchronous rotational state (Black et al. 1995). In-body precession of the spin axis should be observed, but it is not.

It is possible to adjust the moments of inertia such that the precessional period becomes the correct value to return the spin axis to the same position within the body for two of the flybys, but not all three. However, Hyperion's large fraction of voidspace (revealed by its low bulk density) suggests a possible alternate explanation: that the satellite's shape may not necessarily reflect the interior mass distribution, and, thus, correctly predict the principal axes of inertia. We have shown by trying alternate principal axes and moment-of-inertia ratios that a better fit is available after the principal axes are rotated $\sim 30^\circ$ with respect to the shape model's axes, such that the A axis was, in fact, close to the spin axis position in 2005.

Thus, we conclude that it is unlikely that the assumption of homogeneity is valid for Hyperion and, furthermore, that the long and short axes of the shape model are not accurate guides to the principal axes of inertia. A five-dimensional combinational model—one in which both the axis positions and moment-of-inertia ratios are varied—could probably return a better fit (as measured by reduced χ^2) than either the two-dimensional or three-dimensional models shown in Figs. 7 through 11. Given that our best three-dimensional model has a reduced χ^2 of 57, rather than the near-unity expected for an excellent fit, there is room for improvement. However, such a model may not be justifiable by the limited amount of available data (essentially the orientation and spin states at only three epochs), and Hyperion's short Lyapunov time.

Acknowledgments The authors would like to thank Joseph Burns for his helpful comments on drafts and Brian Carcich for assistance with the Hyperion shape model.

References

- Black, G.J., Nicholson, P.D., Thomas, P.C.: Hyperion: rotational dynamics. *Icarus* **117**(1), 149 (1995)
- Duriez, L., Vienne, A.: Theory of motion and ephemerides of Hyperion. *Astron. Astrophys.* **324**, 366 (1997)
- Fowles, G.R., Cassiday, G.L.: *Analytical Mechanics: Sixth Edition*. Thomson Learning Inc., Wadsworth (1999)
- Jacobson, R.A.: Update of the major saturnian satellite ephemerides. JPL Interoffice Memo. 312.1-96-012 (1996)
- Klavetter, J.J.: Rotation of Hyperion II—dynamics. *Astron. J.* **98**, 1855 (1989)
- Melnikov, A.V., Shevchenko, I.I.: On the rotational dynamics of Prometheus and Pandora. *Celest. Mech. Dyn. Astron.* **101**, 31 (2008)
- Peale, S.J.: Origin and evolution of the natural satellites. *Ann. Rev. Astron. Astrophys.* **37**, 533 (1999)

- Thomas, P.C., Armstrong, J.W., Asmar, S.W., Burns, J.A., Denk, T., Giese, B., Helfenstein, P., Iess, L., Johnson, T.V., McEwen, A., Nicolaisen, L., Porco, C.C., Rappaport, N.J., Richardson, J., Somenzi, L., Tortora, P., Turtle, E.P., Veverka, J.: Hyperion's sponge-like appearance. *Nature* **448**, 50 (2007)
- Wisdom, J., Peale, S.J., Mignard, F.: The chaotic rotation of Hyperion. *Icarus* **58**, 137 (1984)